

Hydrated structure of ammonia–water molecule pair via the free energy gradient method: Realization of zero gradient and force balance on free energy surfaces

Yukihiko Nagae, Yuki Oishi, Norihiro Naruse, and Masataka Nagaoka^{a)}

Graduate School of Human Informatics, Nagoya University, Chikusa-ku, Nagoya 464-8601, Japan

(Received 21 February 2003; accepted 24 July 2003)

The hydrated structure of ammonia molecule in aqueous solution was theoretically optimized as an ammonia–water molecule pair ($\text{H}_3\text{N}\cdots\text{H}_2\text{O}$) by the free energy gradient (FEG) method [J. Chem. Phys. **113**, 3516 (2000)]. The interaction between the pair and a solvent water molecule (TIP3P) [J. Chem. Phys. **79**, 926 (1983)] was described by a hybrid quantum mechanical and molecular mechanical method combined with a semiempirical molecular orbital method at the PM3 level of theory. It is concluded that the present FEG method works quite well in spite of a simple steepest descent optimization scheme equipped with the adaptive displacement vector. The free energy stabilization was estimated -0.3 kcal/mol from the free energy for the same structure as that of the cluster in the gas phase. The optimized structure was found to be almost the same as that in the gas phase except for a longer OH bond length of the water molecule. However, its realization in aqueous solution is accomplished by virtue of the fulfillment of both “zero gradient” and “force balance” conditions. Finally, we discuss also the effect of microscopic “solvation entropy,” compared with the result by the conductorlike screening model method. © 2003 American Institute of Physics. [DOI: 10.1063/1.1610436]

I. INTRODUCTION

Recently, the molecular dynamics (MD) method and Monte Carlo (MC) method combined with a hybrid quantum mechanical and molecular mechanical (QM/MM) method have been becoming a prevailing treatment.^{1–11} In particular, for small and medium molecular systems, the so-called *ab initio* MD method is applied to know typical characteristics from a single or a few MD trajectories.^{12,13} On the contrary, for such a large system that concerns essentially some statistical property, the QM/MM-MD method is exclusively utilized at the expense of the chemical accuracy of the electronic property of the QM portion and seeks to resolve not only many-body problems, but also the statistical averaging procedure.

In particular, in solution, such methods that use some semiempirical MO method for the QM portion—e.g., AM1 (Ref. 14) and PM3 (Refs. 15 and 16) levels of theory—have been applied successfully as the effective tools.^{9–11} For example, Sehgal *et al.*⁹ examined the relationship between the aqueous rate acceleration and the transition state geometry for the Claisen rearrangement in aqueous solution and found it consistent with early findings.⁹ Gao and Alhambra¹⁰ calculated the free energy of hydration of chloride ions by the hybrid QM/MM method, which incorporates long-range electrostatic interactions and offers a technique of hybrid QM/MM simulation to study chemical reactions involving ionic species in condensed phases.¹⁰ Cummins and Gready¹¹ determined that a low-barrier hydrogen bond is formed when

the mechanism-based substrate 8-methylpterin binds to dihydrofolate reductase.

In addition, recently, on the basis of the above theoretical development, the free energy gradient (FEG) method has been developed^{17–21} and applied to identify not only molecular stable structures²⁰ (SSs) but also transition states²¹ (TSs) in solution with *full optimization* with respect to all the internal coordinates of solute molecules: e.g., SS in glycine zwitterion^{18–20} and TS in a Menshutkin reaction in aqueous solution.²¹ Being analogous to the energy gradient method for the Born–Oppenheimer potential energy surface (PES) in *ab initio* MO calculations, the FEG method utilizes the force on the FE surface (FES), i.e., the negative FE gradient, in order to identify SSs and TSs. In this article, taking into consideration the previous studies of ammonia–water clusters,^{22–24} the hydrated structure of the ammonia molecule in aqueous solution is theoretically optimized as an ammonia–water molecule pair ($\text{H}_3\text{N}\cdots\text{H}_2\text{O}$) by the FEG method combined with QM/MM-MD calculations.

In Sec. II, the theory and method of calculation are explained: (A) the adopted QM/MM Hamiltonian and Lennard-Jones parameters, (B) the explanation of the present MD method and the conditions of simulation, (C) the free energy perturbation theory^{25,26} and its relation to the present semiempirical QM/MM-MD formalism, and finally (D) the FEG method^{17–21} and the steepest descent optimization scheme with adaptive displacement vector. In Sec. III, we will give a number of results and discussion with respect to (A) the optimized structure of an ammonia–water 1:1 pair in aqueous solution and the free energy of hydration and (B) the hydrated structure and effect of microscopic “solvation entropy.” In particular, in Sec. III B, the present hydrated struc-

^{a)}Author to whom correspondence should be addressed. Fax: +81-52-789-5623. Electronic mail: mnagaoka@info.human.nagoya-u.ac.jp; http://frontier.ncube.human.nagoya-u.ac.jp/

ture is compared with that by the conductor like screening model (COSMO) method,²⁷ and the similar tendency and influence of the glycine hydrated structure are comparatively demonstrated. Finally, in Sec. IV, the main results are summarized with some perspectives in relation to the ionization process of ammonia in aqueous solution.

II. THEORY AND METHOD OF CALCULATION

A. QM/MM method

We adopted a QM/MM method to describe the solution system for the purpose of including the solvent microscopic structures explicitly into the solute electronic states.²⁻⁸ Then, the Hamiltonian of the whole solution system is expressed as

$$\hat{H} = \hat{H}_{\text{QM}} + \hat{H}_{\text{MM}} + \hat{H}_{\text{QM/MM}}, \quad (2.1)$$

where the first two terms \hat{H}_{QM} and \hat{H}_{MM} stand for the standard Hamiltonian of the QM and MM systems while the last QM/MM Hamiltonian $\hat{H}_{\text{QM/MM}}$ holds for the interaction between QM and MM regions. $\hat{H}_{\text{QM/MM}}$ is expressed as a sum of electrostatic and *nonelectrostatic* (van der Waals) contributions:

$$\hat{H}_{\text{QM/MM}} = \hat{H}_{\text{QM/MM}}^{\text{elec}} + \hat{H}_{\text{QM/MM}}^{\text{vdW}}, \quad (2.2)$$

where

$$\hat{H}_{\text{QM/MM}}^{\text{elec}} = \sum_M q_M V_{\text{QM}}(\mathbf{R}_M), \quad (2.3)$$

with

$$V_{\text{QM}}(\mathbf{R}_M) = - \sum_i \frac{1}{r_{iM}} + \sum_A \frac{Z_A}{R_{AM}} \quad (2.4)$$

and

$$\hat{H}_{\text{QM/MM}}^{\text{vdW}} = \sum_A \sum_M \left(\frac{A_{AM}}{R_{AM}^{12}} - \frac{B_{AM}}{R_{AM}^6} \right). \quad (2.5)$$

In these expressions, q_M is the atomic point charge on the M th MM atom, \mathbf{R}_M is the position vector of the M th MM atom, r_{iM} is the distance between the i th QM electron and the M th MM atom, Z_A is the core charge of A th QM atom, R_{AM} is the distance between the A th QM atom and the M th MM one, and A_{AM} and B_{AM} are the Lennard-Jones parameters for the A th QM atom interacting with the M th MM atom.

In the present study, the ammonia-water molecule pair—i.e., H₃N \cdots H₂O—is considered the QM portion and \hat{H}_{QM} in Eq. (2.1) is then described by the PM3 Hamiltonian,^{15,16} while the solvent water molecules were treated molecular mechanically by the TIP3P model²⁸ as the MM molecules that constitute \hat{H}_{MM} in Eq. (2.1).

For the Lennard-Jones-type interaction between QM and MM atoms, as shown in Table I, we have used those parameters developed by Ruiz-López's group especially for a couple of QM ammonia and TIP3P water molecules and a couple of QM and TIP3P water molecules.⁸ Then, the core-core interaction energy between QM and MM atoms was

TABLE I. van der Waals parameters for the PM3/TIP3P potential in the FEG method combined with the QM/MM-MD method.

QM molecule	QM atom	A_{AM} (kcal Å ¹² /mol)	B_{AM} (kcal·Å ⁶ /mol)
H ₂ O	O	2.039×10^2	1.690×10^1
	H	3.355×10^{-6}	1.638×10^{-3}
NH ₃	N	9.038×10^2	1.304×10^2
	H	0.000	0.000

evaluated by the method of Cummins and Gready,²⁹ in which some additional parameters⁶ such as the Ohno-Kloppman factors are set to zero.

B. Molecular dynamics simulation

MD calculations were carried out for a system containing a couple of reactant molecules, i.e., an ammonia and a water molecule, and 241 water molecules in a cubic simulation box ($19.34 \times 19.34 \times 19.34$ Å³) with the periodic boundary condition. The temperature was controlled to 300 K with the Nosé-Hoover chain algorithm³⁰ and the system was maintained to be a canonical (NVT) ensemble. As a result, the mass density in the box was prepared to be 1.0001 g/cm³. The nonbonded cutoff distance was chosen as 9.0 Å. After an equilibration MD run, sampling runs were executed for 3 ps with a time step of 0.1 fs. All the MD calculations were performed with the PM3/TIP3P potential⁸ using ROAR 2.0 (Refs. 31 and 32) partly modified for the present purpose.

C. Free energy perturbation theory

The free energy perturbation (FEP) theory^{25,26} provides us with the FE change ΔG_i , as the H₃N \cdots H₂O geometry \mathbf{q}^s is varied from \mathbf{q}_i^s to \mathbf{q}_{i+1}^s [as is defined later in Eq. (2.10)], which is obtained by

$$\begin{aligned} \Delta G_i &= G_{i+1} - G_i \\ &= -k_B T \ln \langle \exp[-\beta \{V_{\text{RS}}(\mathbf{q}_{i+1}^s) - V_{\text{RS}}(\mathbf{q}_i^s)\}] \rangle_i, \end{aligned} \quad (2.6)$$

where $V_{\text{RS}}(\mathbf{q}_i^s)$ is the sum of the solute potential energy $V_{\text{R}} (= \langle \Psi | \hat{H}_{\text{QM}} | \Psi \rangle)$ and the solute-solvent interaction energies at \mathbf{q}_i^s , and can be represented, in the QM/MM formalism, as

$$V_{\text{RS}} = \langle \Psi | \hat{H}_{\text{QM}} + \hat{H}_{\text{QM/MM}} | \Psi \rangle = V_{\text{R}} + \langle \Psi | \hat{H}_{\text{QM/MM}} | \Psi \rangle, \quad (2.7)$$

where Ψ denotes the instantaneous SCF wave function of electrons of the reactant molecules (\mathbf{q}_i^s) in solution. The brackets $\langle \cdots \rangle$ in Eq. (2.6) denote the time average, which is equal to the equilibrium ensemble average,

$$\langle \cdots \rangle = \frac{\int d\mathbf{q}^B (\cdots) \exp(-\beta V)}{\int d\mathbf{q}^B \exp(-\beta V)}, \quad (2.8)$$

where V is the whole system potential. The subscript i in the average $\langle \cdots \rangle_i$ in Eq. (2.6) means that it is taken over the sampling at \mathbf{q}_i^s .

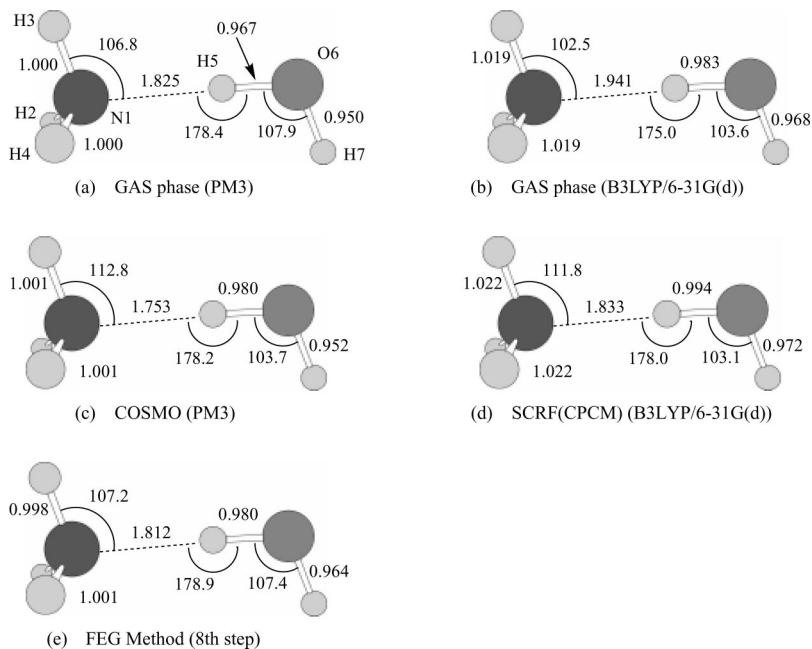


FIG. 1. Optimized geometries of the $\text{HN}_3 \cdots \text{H}_2\text{O}$ complex in the gas phase by (a) the PM3 and (b) B3LYP/6-31G(d) level of theory and in aqueous solution by (c) the COSMO method at the PM3 level, (d) the SCRFF(CPCM) method at the B3LYP/6-31G(d) level of theory, and (e) the FEG method. Bond lengths are in Å and bond angles are in degree.

D. Free energy gradient method

In the MD simulation, the forces acting on each atom of the solute molecule by all solvent molecules are always calculated every time step. By time-averaging the sum of forces acting on each constituent atom of a solute molecule over the equilibrium distribution with respect to all the solvent molecules, the force on FES—i.e., a minus of FEG—is obtained as a function of \mathbf{q}^s as follows:¹⁷

$$\mathbf{F}^{\text{FE}}(\mathbf{q}^s) = - \frac{\partial G(\mathbf{q}^s)}{\partial \mathbf{q}^s} = - \left\langle \frac{\partial V_{\text{RS}}(\mathbf{q}^s)}{\partial \mathbf{q}^s} \right\rangle, \quad (2.9)$$

where $G(\mathbf{q}^s)$ is the FE function.

In the FEG method with the following steepest-descent-path procedure, the $(i+1)$ th reactant structure \mathbf{q}_{i+1}^s is taken to be

$$\mathbf{q}_{i+1}^s = \mathbf{q}_i^s + \Delta \mathbf{q}_i^s, \quad (2.10)$$

where the adaptive displacement vector $\Delta \mathbf{q}_i^s$ is defined as

$$\Delta \mathbf{q}_i^s \equiv c_i \cdot \mathbf{M}^{-1} \cdot \mathbf{F}_i^{\text{FE}}, \quad (2.11)$$

by multiplying

$$\mathbf{F}_i^{\text{FE}} \equiv \mathbf{F}^{\text{FE}}(\mathbf{q}_i^s) = - \left\langle \frac{\partial V_{\text{RS}}(\mathbf{q}^s)}{\partial \mathbf{q}^s} \right\rangle_i, \quad (2.12)$$

by an adaptive constant c_i of dimension T^2 and the inverse of the mass matrix,

$$\mathbf{M} = \begin{pmatrix} m_1 & & & & & & & \\ & m_1 & & & & & & \mathbf{0} \\ & & m_1 & & & & & \\ & & & \ddots & & & & \\ & & & & m_7 & & & \\ \mathbf{0} & & & & & & m_7 & \\ & & & & & & & m_7 \end{pmatrix} \quad (2.13)$$

Since we adopt here the steepest descent method as the geometry optimization method to obtain the stable $\text{H}_3\text{N} \cdots \text{H}_2\text{O}$ structure in aqueous solution, the FEG method procedure is executed in the following processes:

(P1) Start with the geometry \mathbf{q}_k^s , $k=0$.

(P2) For \mathbf{q}_k^s , calculate the free energy change ΔG_k and the force on the FES \mathbf{F}_k^{FE} .

(P3) Find the stationary point using the force

$$\Delta \mathbf{q}_k^s = c_k \cdot \mathbf{M}^{-1} \cdot \mathbf{F}_k^{\text{FE}}. \quad (2.14)$$

If the force \mathbf{F}_k^{FE} is small enough within the tolerance of convergence and/or the predicted change in the geometry $\Delta \mathbf{q}_k^s$ is small enough to be satisfied with the condition

$$\left\langle \frac{\partial V_{\text{RS}}(\mathbf{q}^s)}{\partial \mathbf{q}^s} \right\rangle_k \approx 0, \quad \text{zero-gradient condition}, \quad (2.15)$$

then, stop.

(P4) Set $\mathbf{q}_{k+1}^s = \mathbf{q}_k^s + \Delta \mathbf{q}_k^s$, $k=k+1$ and return to step 2.

III. RESULTS AND DISCUSSION

A. Structure optimization and free energy of hydration

To obtain the most stable structure of the ammonia-water 1:1 pair—i.e., $\text{H}_3\text{N} \cdots \text{H}_2\text{O}$, in aqueous solution—the geometry optimization procedure started from the geometry that was optimized in the gas phase at the PM3 level of theory [Fig. 1(a)], in a similar way to the following steepest-descent-path procedure explained in the preceding section. At each optimization step number i , the atomic positions \mathbf{q}_i^s were updated along the direction of the average force vector $\mathbf{F}^{\text{FE}}(\mathbf{q}_i^s)$ by the displacement vector $\Delta \mathbf{q}_i^s$ that was calculated by Eq. (2.11). During the optimization, the scaling constant c_i was presently varied in the range between 0.1 and $1.0 \text{ au}^2 \text{ \AA}/\text{bohr}$.³³

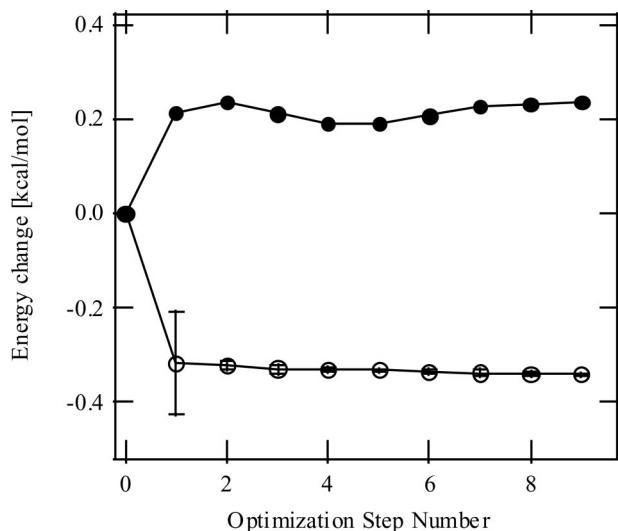


FIG. 2. Free energy change (open circles with an error bar) and solute potential energy change (closed circles) of the stabilization of the ammonia-water 1:1 pair in aqueous solution using the FEG method combined with the QM/MM-MD method at the PM3 level of theory.

In Fig. 2, both ΔG (300 K) and ΔV_R are shown as functions of the step number of optimization—i.e., the optimization step number—which denote the FE change at 300 K and the corresponding change in the solute potential energy V_R ($=\langle\Psi|\hat{H}_{QM}|\Psi\rangle$), respectively. At the first step of optimization, ΔG decreases suddenly to almost -0.3 kcal/mol, while it becomes almost flat up to 9. Presently, judging from the calculated root-mean-square (rms) values [see Eqs. (3.2) and (3.3)], the geometry at optimization step number 8 is taken to be the most stable structure of the ammonia-water molecule pair, and then the FE change of stabilization from the initial geometry results in -0.3 kcal/mol. Here, it is worth noting that the FE change of stabilization—i.e., -0.3 kcal/mol—is such a value that is gained, during geometry optimization, as an FE difference between the FE of the pair immersed at the same shape as the structure optimized in the gas phase at the PM3 level of theory [Fig. 1(a)] and the FE at the optimized geometry of the ammonia-water 1:1 pair in aqueous solution obtained by the FEG method [Fig. 1(e)]. Namely, if we include the FE of solvation from gas to aqueous solution,

$$\begin{aligned}\Delta G_{sol}(\mathbf{q}_0^s) &= \langle V_{RS}(\mathbf{q}_0^s) \rangle_0 - V_R(\mathbf{q}_0^s) \\ &= \langle V_{RS}(\mathbf{q}_0^s) \rangle_0 - \langle \Psi | \hat{H}_{QM}(\mathbf{q}_0^s) | \Psi \rangle,\end{aligned}\quad (3.1)$$

resulting in -27.4 kcal/mol as a difference of -87.0 kcal/mol and -59.6 kcal/mol on the right-hand side, the FE of stabilization thus defined finally becomes -27.7 kcal/mol.

As is shown in Fig. 3(a), the average rms force at an optimization step number i ,

$$\text{rms}(\mathbf{F}_i^{\text{FE}}) = \frac{1}{T} \int_0^T dt \sqrt{[\mathbf{F}_i^{\text{FE}}(t)]^2 / 3N_{atom}}, \quad (3.2)$$

also does not vary with optimization step numbers larger than 1, and is reduced to a half as small as its initial value, at the optimized geometry: i.e., 0.0043 hartree/bohr. Despite the simple optimization scheme adopted here, the present

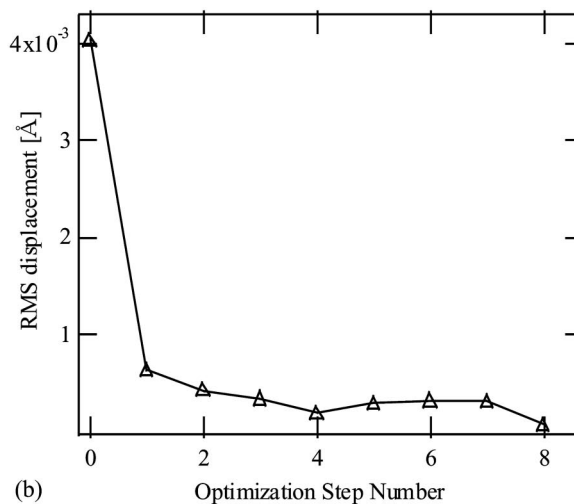
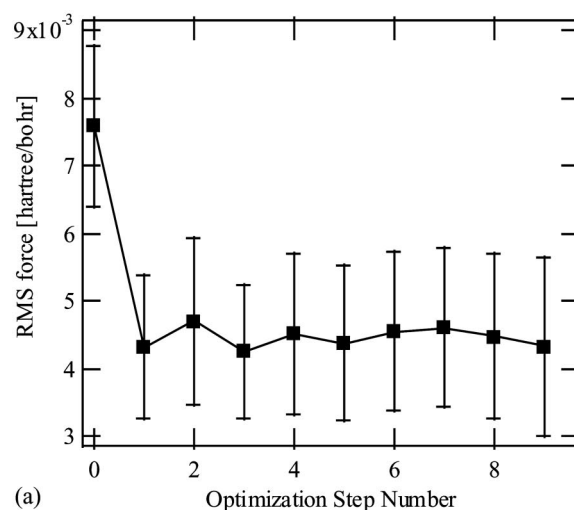


FIG. 3. (a) rms force change and (b) rms displacement on the free energy surface of the ammonia-water 1:1 molecular pair in aqueous solution using the FEG method combined with the QM/MM-MD method at the PM3 level of theory.

value is comparable to 0.0025 hartree/bohr in Ref. 20. In Eq. (3.2), N_{atom} is the total number of atoms—i.e., 7 for the present system—and the upper limit T is 3 ps ($=30\,000$ steps $\times 0.1$ fs)—i.e., the time period for equilibrium MD simulation at a certain structure of the ammonia-water molecule pair.

Similarly, if we define the rms displacement at an optimization step number i as

$$\text{rms}(\Delta \mathbf{q}_i^s) = \sqrt{(\Delta \mathbf{q}_i^s)^2 / 3N_{atom}}, \quad (3.3)$$

the *minimum* rms displacement among those of all successive two optimization steps,

$$\text{rms}(\Delta \mathbf{q}^s) \equiv \min_{\{i\}} \text{rms}(\Delta \mathbf{q}_i^s), \quad (3.4)$$

was found to be 6.339×10^{-5} Å at optimization step number 8 in Fig. 3(b). Finally, at the eighth optimization step number, the ammonia-water molecule pair was judged to be optimized in aqueous solution within an accuracy enough to be satisfied with the condition, Eq. (2.15).

On the other hand, ΔV_R also increases suddenly at the first step (Fig. 2). This means that the destabilization of the solute potential energy V_R is offset by a large hydration energy change. As a result, the stable structure is optimized in compensation for the balance between the solute potential energy gradient and the forces acting on each solute atom due to hydration. Thus, if the optimization might be accomplished exactly, the following condition of force-balance must be fulfilled:

$$\left\langle \frac{\partial V_R(\mathbf{q}^s)}{\partial \mathbf{q}^s} \right\rangle = \left\langle \frac{\partial \langle \Psi | \hat{H}_{QM} | \Psi \rangle}{\partial \mathbf{q}^s} \right\rangle = - \left\langle \frac{\partial \langle \Psi | \hat{H}_{QM/MM} | \Psi \rangle}{\partial \mathbf{q}^s} \right\rangle, \quad (3.5)$$

in addition to Eq. (2.15): i.e., the condition of zero gradient.

B. Hydrated structure

In Fig. 1, the optimized equilibrium geometries in aqueous solution [Figs. 1(c), 1(d), and 1(e)] are also shown in comparison to those in the gas phase [Figs. 1(a) and 1(b)]. They were obtained not only by the FEG method combined with QM/MM-MD calculation [Fig. 1(e)] but also by the COSMO method¹⁷ at the PM3 [Fig. 1(c)] and the B3LYP/6-31G(d) [Fig. 1(d)] level of theory, respectively. For the latter calculation, the polarized continuum model using the polarizable conductor calculation model³⁴ (CPCM), was utilized in GAUSSIAN 98,³⁵ which is a self-consistent reaction field (SCRf) method corresponding to an implementation of the COSMO method in GAUSSIAN 98. All optimized structures show C_s symmetry. In comparison to the experimental value 2.983 Å of $R(N-O)$ in the linear $N \cdots H-O$ hydrogen bond of the $HN_3 \cdots H_2O$ complex,²³ the present values 2.792 and 2.924 Å in the gas phase by the PM3 and B3LYP/6-31G(d) level of theory, respectively, show good agreement.

In those three structures in aqueous solution [Figs. 1(c), 1(d), and 1(e)], it is evident that both O6–H5 and O6–H7 bond lengths of the water molecule become longer than those in the gas phase geometry [Figs. 1(a) and 1(b)], respectively, while the length of the hydrogen bonding N1···H5 becomes shorter in aqueous solution. Moreover, the H5–O6–H7 angles in aqueous solution become smaller than those in the gas phase, respectively. In the COSMO(PM3) and SCRf(CPCM) [B3LYP/6-31G(d)] methods, therefore, the dipole moments as a whole pair—i.e., 4.109 and 4.980 D—were found to be especially larger than those in the gas phase—i.e., 3.485 and 4.178 D, respectively. This tendency is owing to the electronic polarization due to the solvent—namely, due to the “dielectric” hydration—in spite of the solute potential energy destabilization (Fig. 2 and Table II), which is consistent with the opinion about the induced dipole moment of water molecule in water.^{36–38} Actually, under the thermal fluctuation, this polarized state should prepare the next step for the ionization process of ammonia molecule in water: The pair obtains a comparatively larger stabilization energy by its transformation from the polarized state into a ionized state—i.e., a couple of pseudospherical point charges

TABLE II. Atomic charges and dipole moments of the ammonia–water molecule pair.

	COSMO		SCRf(CPCM)		FEG
	PM3	B3LYP/6-31G(d)	PM3	B3LYP/6-31G(d)	
N1	−0.066	−0.907	0.013	−0.951	0.023
H2	0.032	0.317	0.021	0.343	0.017
H3	0.033	0.318	0.021	0.344	0.033
H4	0.038	0.324	0.021	0.343	−0.010
H5	0.226	0.432	0.252	0.436	0.260
O6	−0.436	−0.845	−0.566	−0.905	−0.655
H7	0.174	0.361	0.238	0.390	0.332
Dipole	3.485 ^a	4.178 ^a	4.109 ^a	4.980 ^a	4.004 ^a

^aExpressed in debye.

$(NH_4)^{\delta+}$ and $OH^{\delta-}$ —which are stabilized by the electrostatic interaction with a number of ambient water molecules.

However, in comparison with the COSMO structure at the PM3 level of theory, it is interesting that the geometry change by the FEG method combined with QM/MM-MD calculations is smaller, as a whole, except the O6–H7 bond length. Then, its *apparent* structure may be said to be *rather similar* to that in the gas phase in spite of their different mechanisms of realization. In fact, in the COSMO method—i.e., a dielectric continuum model—the geometry optimization is achieved on the enthalpy basis and, therefore, it cannot take into account legitimately the effect of microscopic “solvation entropy” (SE) that the FEG method combined with QM/MM-MD calculation can.²⁰

In comparison, it is helpful to mention the previous example of the FEG method for an application to obtain the stable structure of glycine zwitterion in aqueous solution,²⁰ where we *did not* utilize the QM/MM method but the empirical valence bond (EVB) potential for describing the interaction potential V_{RS} of glycine and water molecules.¹⁹ The disposable parameters of the EVB potential were optimized to fit a set of 5250 data points of energies and forces calculated by HF/6-31+G(d) level of theory, by a modified Levenberg–Marquardt method for nonlinear least-squares minimization problems.¹⁹ In this example, we also compare the optimized structure in the gas phase by the HF level of theory [Fig. 4(a)] and those in aqueous solution calculated by the FEG method [Fig. 4(b)] and the SCRf(dipole) and SCRf(SCIPCM) methods at the HF/6-31+G(d) level of theory [Figs. 4(c) and 4(d)]. In the latter three structures in aqueous solution, it is evident that those distances between H6 connected to N1 and O5 of the carboxyl group are larger than that in the gas phase geometry, while the C3–O4 bond lengths become larger and the N1–H6 bond length become shorter in aqueous solution. On the other hand, in comparison with both SCRf structures, the geometry change by the FEG method is relatively smaller. These characteristics are very similar to those in the present system of ammonia–water molecule pair ($H_3N \cdots H_2O$) in spite of the totally different interaction model for V_{RS} : i.e., the EVB model.

Thus, in the microscopic descriptive model of water solvent, it should be noticed that the microscopic SE could prevent water molecules from hydrating strongly the whole $H_3N \cdots H_2O$ pair, while the local hydrogen bonding between

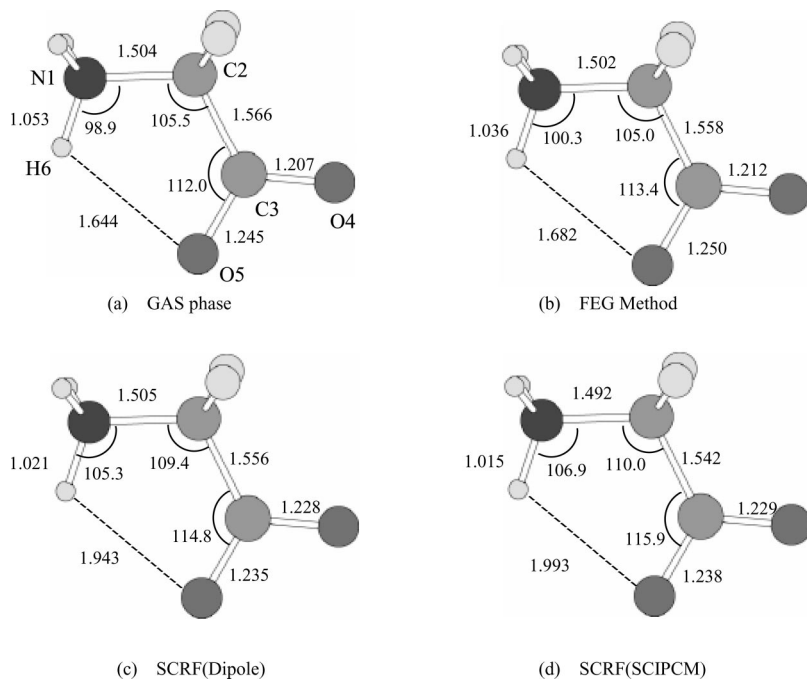


FIG. 4. Optimized geometries of glycine zwitterion in the gas phase by (a) the HF level of theory and in aqueous solution obtained by (b) the FEG method and (c) the SCRf(Dipole) and (d) SCRf(SCIPCM) methods at the HF/6-31 + G(d) level of theory. Bond lengths are in Å and bond angles are in degree.

H7 and an oxygen atom of an ambient water molecule is expected to become stronger than that in the continuum approximation of solvent where the “enthalpic” stabilization is mainly considered but the microscopic SE is not taken explicitly into consideration. In the present $\text{H}_3\text{N}^+\cdots\text{H}_2\text{O}$ pair system, the difference in between the continuum model and the FEG method results in the relatively longer O6–H7 bond length in the latter method. This is the same characteristic with the longer C3–O5 bond length in the stable structure of glycine zwitterion.¹⁹

IV. SUMMARY

In this article, we have obtained and studied the most stable structure of the ammonia–water 1:1 pair—i.e., $\text{H}_3\text{N}^+\cdots\text{H}_2\text{O}$ —in aqueous solution, by the FEG method combined with the QM/MM-MD method at the PM3 level of theory. The free energy stabilization was -0.3 kcal/mol from the free energy of the pair with the same structure as that of the cluster optimized in the gas phase. The present FEG method worked quite well in spite of a simple steepest descent optimization scheme equipped with only the adaptive displacement vector.

The structure of the pair $\text{H}_3\text{N}^+\cdots\text{H}_2\text{O}$ in aqueous solution was found to be almost the same as that in the gas phase except a longer OH bond length of the water molecule whose H atom is hydrogen bonding not to the nitrogen atom of the ammonia molecule but to an oxygen atom in an ambient water molecule. However, its realization in aqueous solution is accomplished by virtue of both subtle fulfillments of the “zero gradient” [Eq. (2.15)] and “force balance” [Eq. (3.5)] conditions. Hence, even if both structures in gas and solution might be sometimes the same, the mechanisms to maintain the structure should be naturally different from each other.

Finally, it is worth noting that, according to our experience of the FEG method,^{17–21} it would be possible using the FEG method to optimize the ionized state—i.e.,

$\text{NH}_4^+\cdots\text{OH}^-$ —in aqueous solution. Then, one could estimate ΔG_{ion} —i.e., the free energy change of ionization of ammonia in aqueous solution—and it would realize to evaluate directly the numerical accuracy of the present FEG methodology through comparing the theoretical value with that obtained experimentally. We are now in applying the FEG method directly for such a purpose stated above.³⁹

ACKNOWLEDGMENTS

The authors thank Professor Manuel F. Ruiz-López for his kind and valuable comments. The numerical calculations were performed partly on Fujitsu VPP800/63 and other machines at the Academic Center for Computing and Media Studies of Kyoto University. This work was supported mainly by a Grant-in-Aid for Science Research from the Ministry of Education, Science and Culture in Japan.

¹J. Gao, *Acc. Chem. Res.* **29**, 298 (1996).

²A. Warshell and M. Levitt, *J. Mol. Biol.* **103**, 227 (1976).

³U. C. Singh and P. A. Kollman, *J. Comput. Chem.* **7**, 718 (1986).

⁴P. A. Bash, M. J. Field and M. Karplus, *J. Am. Chem. Soc.* **109**, 8092 (1987).

⁵A. Warshell, *Computer Modeling of Chemical Reactions in Enzymes and Solutions* (Wiley, New York, 1991).

⁶M. J. Field, P. A. Bash, and M. Karplus, *J. Comput. Chem.* **11**, 700 (1990).

⁷J. Gao and X. Xia, *J. Am. Chem. Soc.* **115**, 9667 (1993).

⁸F. J. Luque, N. Reuter, A. Cartier, and M. F. Ruiz-López, *J. Phys. Chem. A* **104**, 10 923 (2000).

⁹A. Sehgal, L. Shao, and J. Gao, *J. Am. Chem. Soc.* **117**, 11337 (1995).

¹⁰J. Gao and C. Alhambra, *J. Chem. Phys.* **107**, 1212 (1997).

¹¹P. L. Cummins and J. E. Gready, *J. Mol. Graphics Modell.* **18**, 42 (2000).

¹²T. D. Sewell, D. L. Thompson, J. D. Gezelter, and W. H. Miller, *J. Chem. Phys.* **193**, 512 (1992).

¹³H. Yamataka, M. Aida, and M. Dupuis, *Chem. Phys. Lett.* **300**, 583 (1999).

¹⁴M. J. S. Dewar, E. G. Zoebisch, E. F. Healy, and J. J. P. Stewart, *J. Am. Chem. Soc.* **107**, 3902 (1985).

¹⁵J. J. P. Stewart, *J. Comput. Chem.* **10**, 209 (1989).

¹⁶J. J. P. Stewart, *J. Comput. Chem.* **10**, 221 (1989).

- ¹⁷N. Okuyama-Yoshida, M. Nagaoka, and T. Yamabe, *Int. J. Quantum Chem.* **70**, 95 (1998).
- ¹⁸M. Nagaoka, N. Okuyama-Yoshida, and T. Yamabe, *J. Phys. Chem. A* **102**, 8202 (1998).
- ¹⁹N. Okuyama-Yoshida, M. Nagaoka, and T. Yamabe, *J. Phys. Chem. A* **102**, 285 (1998).
- ²⁰N. Okuyama-Yoshida, K. Kataoka, M. Nagaoka, and T. Yamabe, *J. Chem. Phys.* **113**, 3519 (2000).
- ²¹H. Hirao, Y. Nagae, and M. Nagaoka, *Chem. Phys. Lett.* **348**, 350 (2001).
- ²²H. Shinohara, U. Nagashima, H. Tanaka, and N. Nishi, *J. Chem. Phys.* **83**, 4183 (1985).
- ²³P. Herbine and T. R. Dyke, *J. Chem. Phys.* **83**, 3768 (1985).
- ²⁴J. E. Bertie and M. R. Shehata, *J. Chem. Phys.* **83**, 1449 (1985).
- ²⁵R. W. Zwanzig, *J. Chem. Phys.* **22**, 1420 (1954).
- ²⁶U. C. Singh, F. K. Brown, P. A. Bash, and P. A. Kollman, *J. Am. Chem. Soc.* **109**, 1607 (1987).
- ²⁷A. Klamt and G. Schüürmann, *J. Chem. Soc., Perkin Trans. 2* **2**, 799 (1993).
- ²⁸W. L. Jorgensen, J. Chandrasekhar, J. D. Madura, R. W. Impey, and M. L. Klein, *J. Chem. Phys.* **79**, 926 (1983).
- ²⁹P. L. Cummins and J. E. Gready, *J. Comput. Chem.* **18**, 1496 (1997).
- ³⁰G. J. Martyna and M. L. Klein, *J. Chem. Phys.* **97**, 2635 (1992).
- ³¹A. Cheng, R. S. Stanton, J. J. Vincent *et al.*, ROAR 2.0, The Pennsylvania State University, 1999.
- ³²D. A. Pearlman, D. A. Case, J. W. Caldwell *et al.*, AMBER 6.0, University of California, San Francisco, 1995.
- ³³amu is the abbreviation of *atomic time unit*, which is equal to $\text{amu}^{1/2} \text{ bohr hartree}^{-1/2}$.
- ³⁴V. Barone and M. Cossi, *J. Phys. Chem. A* **102**, 1995 (1998).
- ³⁵M. J. Frisch *et al.*, GAUSSIAN 98 Revision A.7, Gaussian, Inc., Pittsburgh, PA, 1998.
- ³⁶J. Gao and X. Xia, *Science* **258**, 631 (1992).
- ³⁷Y. Tu and A. Laaksonen, *Chem. Phys. Lett.* **329**, 283 (2000).
- ³⁸K. Coutinho *et al.*, *Chem. Phys. Lett.* **369**, 345 (2003).
- ³⁹Y. Nagae, Y. Oishi, and M. Nagaoka (unpublished).